Study of Bandwidth and Resonant Frequency of a Rectangular Superconducting Thin Film Patch Antenna at Temperatures near *Tc*

Abdelkrim Belhedri [1], Abderraouf Messai [1], Tayeb A. Denidni [2], and Boualem Mekimah [1]

[1] Electronics Department, Frères Mentouri University, 25000, Constantine, Algeria
belhedri.abdelkrim@umc.edu.dz, r_messai@yahoo.fr, b_mekimah@umc.edu.dz

[2] EMT INRS Montreal Canada
denidni@emt.inrs.ca

Abstract ─ Our work presents a study of High Temperature Superconductor (HTS) Yttrium Barium Copper Oxide YBaCuO rectangular thin film. It is considered to be etched on lanthanum aluminate (LaAlO3) substrate. Results are exhibited for different values of temperature and patch thickness. Validated and compared to those in literature, these results show direct proportionality between patch thickness and both of resonant frequency and bandwidth for temperatures relatively far from the critical temperature T_C. When temperature becomes very close to T_C, proportionality between resonant frequency and patch thickness is maintained; but it is inverted between bandwidth and patch thickness. Bandwidth is broadened at low values of thickness, but it decreases considerably when thickness increases.

Index Terms ─ Bandwidth, critical temperature, film thickness, high temperature superconductor, patch thickness, resonant frequency, superconductor antennas.

I. INTRODUCTION

HTS antennas show considerable improvement over identical antennas made with their normal metal counterparts [1-3]. A 4-element array in [1] presents a gain 0.9 dB for a direct-coupled feed and 1.7 dB for a gap coupled one. A 100-element array in [4] shows an improvement of 8 to 10 dB. Superconductor antennas have shown certain superiority against conductor antennas, because of their small losses, reduced time of propagation, and large scale of integration [3], [5-6]. Despite having higher gain compared to conductor antennas, their narrow bandwidth severely limits their application [2]. They could be used for RF applications in deep-space, where temperatures are very low [7-8] and do not need to have cooling systems.

Working at temperatures very close to high temperature of transition, using superconductor thin films, allow a big scale of integration relatively to conductors [9]. Bandwidth enhancement has been shown when working with thin films at temperatures near to the critical temperature T_C [10].

Some planar microwave circuits, such as patch antennas [1] and resonators [11-12], fabricated on lanthanum aluminate substrates have shown substantial improvement over identical circuits fabricated with gold, silver, or copper metallization.

Our work is a study of a rectangular YBaCuO thin film supposed to be etched on a LaAlO3 substrate. As mentioned by [1], the LaAlO3 is used in the experiment because of its good lattice match with HTS like YBCO films having low surface impedance and T_C =90K.

First, a mathematical formulation of the problem, based on the Method of Moments (MoMs) is realized. A system of linear equations that leads to an impedance matrix is used to determine the resonant frequency (f_r) and the bandwidth (*BW*), where a non-trivial solution to the impedance matrix is imposed. The obtained results show a big agreement between our results and the experimental results in [1].

Second, a focus on the variations of f_r and *BW* in function of the patch thickness is done. Theses variations are very important when the temperature moves towards T_C. Temperature must be maintained constant in order to keep both of resonant frequency and bandwidth constant; because at this region, near to the critical temperature, the variations of f_r and *BW* are very important. In other words, any small shift in temperature will induce a significant shift of f_r and *BW*.

II. MATHEMATICAL FORMULATION

The studied structure is shown in Fig. 1. It consists of a rectangular high Temperature Superconductor (HTS) YBaCuO thin film, of dimensions *L* and *W*. It has a thickness t and it is supposed to be etched on lanthanum aluminate (LaAlO3) of thickness h. The full-wave method of Moments is used to analyze this structure.

In spectral domain, transverse electric field $\tilde{\tilde{E}}$ on the patch is function of Green tensor $\bar{\bar{G}}$, and current density

Submitted On: April 25, 2018
Accepted On: October 19, 2018

$\tilde{\vec{J}}$ on the patch [3]:

$$\tilde{\vec{E}} = \begin{bmatrix} \tilde{E}_x \\ \tilde{E}_y \end{bmatrix} = \begin{bmatrix} G_{xx} & G_{xy} \\ G_{yx} & G_{yy} \end{bmatrix} . \begin{bmatrix} \tilde{J}_x \\ \tilde{J}_y \end{bmatrix}. \quad (1)$$

In free space, electric field is obtained by using the inverse Fourier transform of $\tilde{\vec{E}}$ as follows:

$$E_x(x,y) = \frac{1}{4\pi^2} \iint_{-\infty-\infty}^{+\infty+\infty} [G_{xx}.\tilde{J}_x + G_{xy}.\tilde{J}_y] e^{+i(k_x x + k_y y)}\, dk_x dk_y, \quad (2a)$$

$$E_y(x,y) = \frac{1}{4\pi^2} \iint_{-\infty-\infty}^{+\infty+\infty} [G_{yx}.\tilde{J}_x + G_{yy}.\tilde{J}_y] e^{+i(k_x x + k_y y)}\, dk_x dk_y. \quad (2b)$$

Using the method of moments - Galekin - procedure - current distribution on the patch is developed into series of known base functions; J_{xn}, J_{ym}; with unknown coefficients, a_n and b_m [13],

$$J_x(x,y) = \sum_{n=1}^{N} a_n J_{xn}(x,y),$$

and

$$J_y(x,y) = \sum_{m=1}^{M} b_m J_{ym}(x,y).$$

The following impedance matrix is obtained after mathematical manipulations in the previous relations:

$$\begin{bmatrix} (Z^1_{kn})_{N\times N} & (Z^2_{km})_{N\times M} \\ (Z^3_{ln})_{M\times N} & (Z^4_{lm})_{M\times M} \end{bmatrix} \begin{bmatrix} (a_n)_{N\times 1} \\ (b_m)_{M\times 1} \end{bmatrix} = \begin{bmatrix} \bar{0} \\ \bar{0} \end{bmatrix}, \quad (3)$$

with: $k,n = \overline{1,N}$; $l,m = \overline{1,M}$ and,

$$Z^1_{kn} = \iint_{-\infty-\infty}^{+\infty+\infty} \tilde{J}_{xk}(-k_x,-k_y).G_{xx}.\tilde{J}_{xn}(k_x,k_y)\, dk_x dk_y,$$

$$Z^2_{km} = \iint_{-\infty-\infty}^{+\infty+\infty} \tilde{J}_{xk}(-k_x,-k_y).G_{xy}.\tilde{J}_{ym}(k_x,k_y)\, dk_x dk_y,$$

$$Z^3_{ln} = \iint_{-\infty-\infty}^{+\infty+\infty} \tilde{J}_{yl}(-k_x,-k_y).G_{yx}.\tilde{J}_{xn}(k_x,k_y)\, dk_x dk_y,$$

$$Z^4_{lm} = \iint_{-\infty-\infty}^{+\infty+\infty} \tilde{J}_{yl}(-k_x,-k_y).G_{yy}.\tilde{J}_{ym}(k_x,k_y)\, dk_x dk_y.$$

A rectangular cavity, with lateral magnetic walls and TM_{01} mode, are considered [13]:

$$J_{xn}(x,y) = sin\left[\frac{n_1\pi}{L}\left(x+\frac{L}{2}\right)\right] cos\left[\frac{n_2\pi}{W}\left(y+\frac{W}{2}\right)\right], \quad (4a)$$

$$J_{ym}(x,y) = sin\left[\frac{m_2\pi}{W}\left(y+\frac{W}{2}\right)\right] cos\left[\frac{m_1\pi}{L}\left(x+\frac{L}{2}\right)\right]. \quad (4b)$$

In case of superconductivity, tangential components of the electric field on the patch are [3]:

$$\begin{cases} E^o_x(x,y,z) = Z_s.J_x(x,y) \\ E^o_y(x,y,z) = Z_s.J_y(x,y) \end{cases}, \quad (5)$$

where, "o" indicates the outside of the patch, J the surface current density, and Z_s the patch surface impedance. According to Gorter and Casimir, Z_s can be expressed as [14]:

$$Z_s = \frac{1}{t.\sigma_n}, \quad \text{and} \quad \lambda = \lambda_0 \left[1 - \left(\frac{T}{T_c}\right)^4\right]^{-\frac{1}{2}}, \quad (6)$$

λ_0 is the penetration depth at 0 K, and σ_n the normal state conductivity. After manipulations we obtain:

$$\begin{bmatrix} \tilde{E}_x(k_x,k_y) \\ \tilde{E}_y(k_x,k_y) \end{bmatrix} = \begin{bmatrix} (G_{xx}-Z_s) & G_{xy} \\ G_{yx} & (G_{yy}-Z_s) \end{bmatrix} . \begin{bmatrix} \tilde{J}_x(k_x,k_y) \\ \tilde{J}_y(k_x,k_y) \end{bmatrix}. \quad (7)$$

A non-trivial solution of (3), when G_{xx} and G_{yy} are respectively replaced by $G_{xx} - Z_s$ and $G_{yy} - Z_s$ of equation (7), implies that [13-14]:

$$det[Z(f)] = 0. \quad (8)$$

The complex resonant frequency is,

$$f = f_r + if_i\,, \quad (9)$$

where, f_i and f_r are respectively imaginary part and real part of resonant the frequency. The bandwidth is:

$$BW = \frac{2f_i}{f_r}\,. \quad (10)$$

III. RESULTS

Dimensions and characteristics of the patch antenna, in Fig. 1 are: $L = 1.63\ mm, W = 0.935\ mm$, film critical temperature $Tc = 89\ K$, and LaAlO3 thickness $h = 0.254\ mm$. The film thickness t is supposed to vary from 10 nm up to 350 nm, $\lambda_0 = 140\ nm$, and $\sigma_n = 10^6\ Sm^{-1}$. The relative permittivity value $\varepsilon_r = 23.3459$ is taken from the curve in Fig. 2 at $T = 50\ K$.

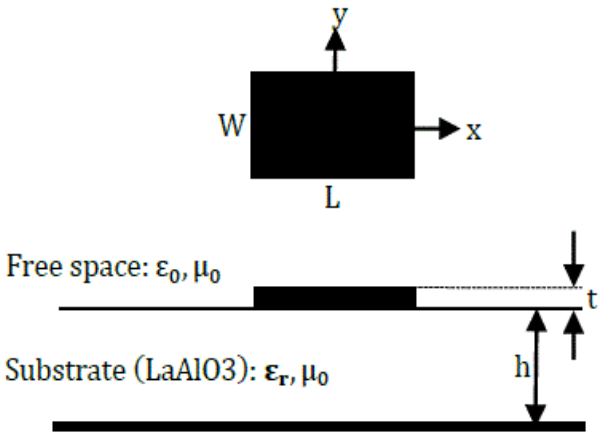

Fig. 1. Structure geometry of the studied antenna.

Based on the theoretical formulation in Section II, our problem is modeled and computed results; according to (8), (9), and (10); are compared to those measured in [1]. They are found to be in good agreement as it is mentioned in Table 1. It is clear that, at $T = 50\ K$, there is an error of 0.84 % between our computed gold and that measured in [1]. Similarly, there is 1.3 % of error between our computed HTS and the measured in [1].

Table 1: Our results compared to [1]

$T_C = 89\ K, T = 50\ K, t = 350\ nm, \lambda_0 = 140\ nm$, $\varepsilon_r = 23.3459, \sigma_n = 10^6\ Sm^{-1}$, and $\sigma_{gold} = 44.2 \times 10^6\ Sm^{-1}$

Our Results		**[1]**		
Resonant Frequency (GHz)		**Resonant Frequency (GHz)**		
Modeled		**Modeled**	**Measured**	
Gold	HTS	HTS	Gold	HTS
29.043	29.039	28.912	29.290	28.667

Measured values of resonant frequencies for either gold and HTS and the relative permittivity of LaAlO3 variations are represented in Fig. 2. They are extracted from direct coupled curves of [1].

Our computed results are represented in Fig. 2 in order to compare them with the measured values. Both of gold electrical conductivity and LaAlO3 relative permittivity variations in function of temperature variations are taken into consideration. It is clear that the relative permittivity of LaAlO3 is proportional to temperature. The computed values of resonant frequency of Gold decrease slowly in the same manner as the measured ones with a slight down shift of about less than 0.25 GHz as the temperature increases. This decrease is because of the slow increase of the relative permittivity with temperature. As for Gold, the HTS computed values vary in the same manner as the measured ones with a shift up of about 0.372 GHz. In Fig. 3, temperature is first, maintained at 40 K then at 70 K. The thickness is varied from 10 nm up to 350 nm. It can be seen that both of resonant frequencies and bandwidths, for the above temperatures, present a small increase as patch thickness increases. This increase is relatively rapid around 10 nm thickness.

For temperatures very close to T_C, the resonant frequency continues to increase when thickness increases. A rapid increase is visible in Fig. 4 when thickness is less than 50 nm. On the other hand, the bandwidth decreases rapidly when the film thickness increases. This decrease is accentuated for values of thickness less than 100 nm at $T = 88.9$ K. This accentuation decreases as the temperature shifts down T_C. Taking into consideration the relative permittivity value for each value of temperature, typical values of temperature and the corresponding values of resonant frequency and bandwidth are summarized in Table 2.

We notice, for a $10\ nm$, that the bandwidth increases from 5.05% to 41.085%, while the resonant frequency decreases from 24.569 GHz to 16.567 GHz when the temperature increases from 88.5 K to 88.9 K.

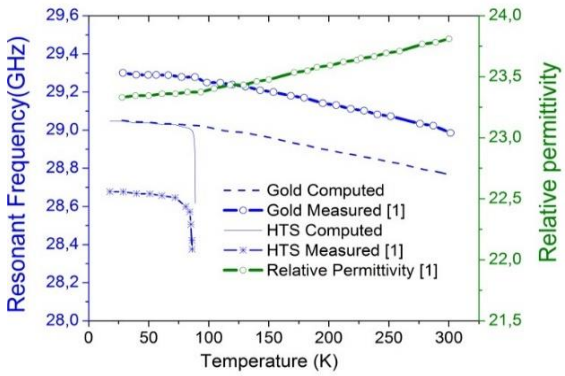

Fig. 2. LaAlO3 relative permittivity, resonant frequency in GHz for Gold and HTS in function of temperature $Tc = 89$ K, $\lambda_0 = 140$ nm, $t = 350$ nm, $\sigma_n = 10^6\ Sm^{-1}$, and $\sigma_{gold} = 44.2 \times 10^6\ Sm^{-1}$.

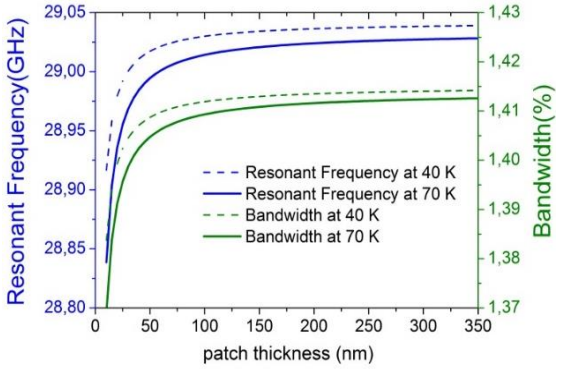

Fig. 3. Resonant frequency, bandwidth variations in function of patch thickness at 40 K and 70 K, $Tc = 89$ K, $\lambda_0 = 140$ nm, and $\sigma_n = 10^6\ Sm^{-1}$.

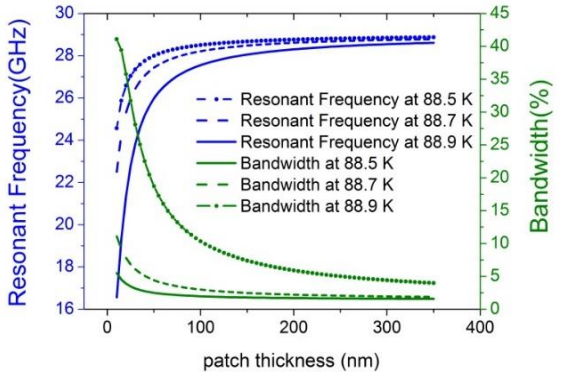

Fig. 4. Resonant frequency, bandwidth variations versus patch thickness at 88.5 K, 88.7 K, and 88.9 K, $Tc = 89$ K, $\lambda_0 = 140$ nm, and $\sigma_n = 10^6\ Sm^{-1}$.

The bandwidth drops drastically when the temperature shifts down the high temperature of transition.

Table 2: Resonant frequency and bandwidth typical values at different values of temperature and relative permittivity

$Tc = 89\ K, t = 10\ nm\ \lambda_0 = 140\ nm,$ and $\sigma_n = 10^6\ Sm^{-1}$

T (K)	ε_r	Resonant Frequency (GHz)	BW (%)
88.9	23.375	16.567	41.085
88.7	23.375	22.509	11.082
88.5	23.375	24.569	5.505
70	23.3605	28.839	1.369
40	23.3459	28.917	1.384

IV. CONCLUSION

Our results show that there is a direct proportionality between patch thickness and both of resonant frequency and bandwidth at temperatures relatively far from T_C. Contrarily to temperatures near to T_C, this proportionality is inverted between bandwidth and patch thickness. This inversion occurs when temperature moves towards the critical temperature T_C, depending on both of temperature and patch thickness. In perspective, research works are in progress to determine the relationship between temperature, patch thickness, and the inversion of proportionality.

REFERENCES

[1] M. A. Richard, K. B. Bhasin, and P. C. Claspy, "Superconducting microstrip antennas: An experimental comparison of two feeding methods," *IEEE Transactions on Antennas and Propagation*, vol. 41, no. 7, July 1993.

[2] S. Liu and B. Guan, "Wideband high-temperature superconducting microstrip antenna," *Electronics Letters*, vol. 41, no. 17, Aug. 2005.

[3] T. Fortaki, M. Amir, S. Benkouda, and A. Benghalia, "Study of high Tc superconducting microstrip antenna," *Piers Online*, vol. 5, no. 4, 2009.

[4] R. J. Dinger, "Some potential antenna applications of high temperature superconductors," *J. Superconductivity*, vol. 3, no. 3, pp. 287-296, Sept. 1990.

[5] S. Bedra, T. Fortaki, A. Messai, and R. Bedra, "Spectral domain analysis of resonant characteristics of high Tc superconducting rectangular microstrip patch printed on isotropic or uniaxial anisotropic substrates," *Wireless Personal Communications*, Springer, July 2015.

[6] A. Messai, S. Benkouda, M. Amir, S. Bedra, and T. Fortaki, "Analysis of high Tc superconducting rectangular microstrip patches over ground planes with rectangular apertures in substrates containing anisotropic materials," *International Journal of Antennas and Propagation*, 2013.

[7] N. Chahat, J. Sauder, R. E. Hodges, M. Thomson, and Y. Rahmat-Samii, "The deep-space network telecommunication CubeSat antenna using the deployable Ka-band mesh reflector antenna," *IEEE Antennas and Propagation Magazine*, vol. 59, no. 4, Apr. 2017.

[8] S.-H. Hong, G.-B. Choi, R.-H. Baek, H.-S. Kang, S.-W. Jung, and Y.-H. Jeong, "Low-temperature performance of nanoscale MOSFET for deep-space RF applications," *IEEE Electron Device Letters*, vol. 29, no. 7, July 2008.

[9] A. Belhedri, A. Messai, and B. Mekimah, "Miniaturization of microstrip patch antennas using superconducting thin films at the high temperature of transition," *5th International Conference on Information and Communication Systems (ICICS)*, 2014.

[10] A. Belhedri, A. Messai, and B. Mekimah, "Performance amelioration of microstrip patch antennas using thin films at the high temperature of transition," *Science and Information Conference*, London, UK, Aug. 2014.

[11] C. M. Chorey, K. Kong, K. B. Bhasin, J. D. Warner, and T. Itoh, "YBCO superconducting ring resonator at millimeter-wave frequencies," *IEEE Trans. Microwave Theory Tech.*, vol. 39, pp. 1480-1487, Sept. 1991.

[12] J. H. Takemoto, F. K. Oshita, H. R. Fetterman, P. Korbin, and E. Sovoro, "Microstrip ring resonator technique for measuring microwave attenuation in high-Tc superconducting thin films," *IEEE Trans. Microwave Theory Tech.*, vol. 37, pp. 1650-1652, 1989.

[13] T. Fortaki, D. Khedrouche, F. Bouttout, and A. Benghalia, "Anumerically efficient full-wave analysis of a tunable rectangular microstrip patch," *Int. J. Electronics*, vol. 91, no. 1, Jan. 2004.

[14] T. Fortaki, S. Benkouda, M. Mounir, and A. Benghalia, "Air gap tuning effect on the resonant frequency and half-power bandwidth of superconducting microstrip patch," *Piers Online*, vol. 5, no. 4, 2009.